accepted to appear in the Proceedings of the IEEE Transportation Electrification Conference in June 19-21, 2019 in Novi, MI.

A Flexible V2V Charger as a New Layer of Vehicle-Grid Integration Framework

Emin Ucer[1], Ramona Buckreus[1], Mithat C. Kisacikoglu[1], Eyuphan Bulut[2], Mustafa Guven[3], Yilmaz Sozer[4], Luigi Giubbolini[5]
[1]Dept. of Electrical and Computer Eng., University of Alabama, Tuscaloosa, AL
[2]Dept. of Electrical and Computer Eng., Virginia Commonwealth University, Richmond, VA
[3]Caterpillar Inc., Mossville, IL
[4]Dept. of Electrical and Computer Eng., University of Akron, Akron, OH
[5]Andromeda Power LLC, Long Beach, CA

***Abstract*—This study proposes a flexible and marketable electric vehicle-to-electric vehicle (V2V) charge sharing solution that will lead to faster and wider customer adoption of electric vehicles (EVs) as an alternative to current grid-to-vehicle charging methodologies. The energy transfer between EVs will be through a bidirectional DC-DC converter in a conductive way which can take place at parking lots of workplaces, campuses, or residential premises and highways. The proposed design provides compact infrastructure, wide input and output voltage ranges with bidirectional buck/boost operation, and fast power transfer compared to Level 2 charging stations. To demonstrate this idea, this study evaluated three different bidirectional DC-DC converter topologies and validated the developed prototype with experimental results. We further analyzed V2V energy sharing in terms of impact on new charging station installations and possible grid services that can be provided.**

I. Introduction

Today, real-time charging from the utility grid is recognized to be the mainstream way of 'fueling' electric vehicles (EVs). However, since the current EV penetration rates are very limited, many of the problems such as increased distribution level peak demand [1]–[3] tied to grid-integration of EVs are not clearly differentiated. Studies show that residential EV charging will result in disruptive problems in the distribution grid of the future [1]–[8]. This indicates that residential EV charging must be accompanied by faster public stations to sustain the EV growth. Therefore, approximately 40 million EVs expected to be on the road in the US by 2030 will require 400K new DC fast charging (DCFC) outlets [9]. Furthermore, an average US driver operates his/her vehicle 59.69 min per day [10] and requests DCFC mainly around noon and between 3pm-6pm [11]. Consequently, to respond this tight spatio-temporal charging request within a city, more than $90K upfront cost per DCFC station is needed [12]. Furthermore, issues around land ownership, municipal permitting, electrical grid limitations and other factors have slowed the DCFC installations [13].

In this study, we propose a vehicle-to-vehicle (V2V) Charge Sharing Network (CSN) philosophy to provide an alternative, more convenient, and flexible way of conducting EV charging. The design and implementation of V2V CSN will greatly reduce the range anxiety of EVs with minimal infrastructure cost. The proposed solution has the potential to provide an invaluable service that will benefit EV owners, local communities and municipalities, and the utility grid, especially as a demand response management tool during peak-times.Such a scenario is very viable since most EV owners charge their EVs daily at home after only using it for 25–30 miles of commute; they have, therefore, on average about 50–60% of their battery capacity available to sell [14]. V2V CSN will allow users (either battery EV, plug-in hybrid, or fuel-cell EV) with unused electric energy on their board to connect with users who need charge at comparable transfer rates to fast charging stations.

V2V charging requires an analysis both in terms of how to match suppliers to receivers with efficient matching algorithms and how to enable energy exchange with current EV charging technologies. Authors previously developed a Java-based simulation tool to analyze the viability of the proposed V2V CSN technology [15]. The tool generates a customizable simulation environment with different parameters including EV types and counts, charging station types and locations, and user mobility patterns. Although the literature is limited on this developing topic, some recent papers addressed the challenges surrounding energy sharing between EVs. In [16], authors present a matching algorithm to facilitate V2V cooperative energy transfer. It compares two different V2V matching algorithms with traditional grid-based charging. In [17], the matching of demander EVs to both V2V suppliers and existing charging stations has been studied in an efficient and privacy preserving manner. In [18], an authentication protocol between vehicles before they actually start V2V charging has been presented.

On the other hand, the concept of dc-dc power conversion for automotive applications has been addressed in the literature for various applications [19], [20]. Recently, three different solutions for V2V energy transfer have been compared in [21]: vehicle-to-grid and grid-to-vehicle (V2G+G2V), V2V over direct ac interconnection (acV2V), and V2V over dc interconnection (dcV2V). It is shown that dcV2V is more efficient than the other options due to reduced number of energy conversions. Moreover, a combined half-bridge (CHB) type converter is used for dcV2V which had previously been reported in [22]. In [22], mobile charging with an energy

Fig. 1. A Nissan Leaf is transferring energy to a Tesla Model S through a conductive charging cable. A mobile app communicating with both vehicles lets the drivers control the charging process [24], [26]

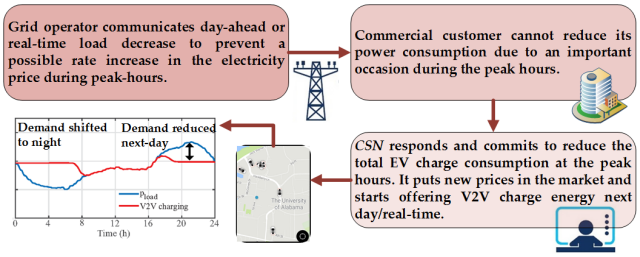

Fig. 2. V2V charging mechanism based on power system operation.

storage device using a three-phase, interleaved, bidirectional, cascaded buck-boost (CBB) dc-dc converter was reported and compared with CHB design counterpart. However, the study does not completely outline technical challenges and design procedures specific to V2V energy transfer. A converter design is also proposed in [23] which allows four common energy transfer modes which are V2G, G2V, vehicle-to-home (V2H), and V2V. The paper focuses on higher power density design with efficient operation for the above operation modes. V2V operation proposed in [23] proposes to use on-board chargers which limits the speed of energy transfer.

As a practical industry example, Fig. 1 shows the V2V charging realized by Andromeda Power using 'Orca Inceptive' [24]. This product is rated at 50 kW and designed as a mobile charging station that also supports charging from the grid. The hardware can be seen in the trunk of a Nissan Leaf in Fig. 1. The charging process can also be controlled via a mobile app as shown in Fig. 1. The proposed V2V charger in this study will also communicate with the grid over an app similar to the one shown in Fig. 1. The app will help matching of demanders to suppliers, controlling the energy exchanged, and completing the required transactions. For demanders, the app will display on a map the available supplier EVs in the vicinity, with information on the energy amount that could be supplied. This map will mainly show and reassure that there are potential suppliers. However, the actual matching of suppliers to demanders will be done by a server, after the demander requests for service (similar to the Uber platform [25]). After the server assigns a supplier to the demander, the supplier EV will come nearby and get connected via a bi-directional dc-dc converter.

The unique challenge of this study different from the literature is that the supplier and receiver voltages vary greatly depending on the battery state of charge (SOC) levels and can even overlap each other during the energy sharing. Furthermore, the V2V charger will need to be directionally agnostic providing utmost flexibility for the customer usage so that any side of the V2V charger can be supplier/receiver.

Our main contributions in this paper can be summarized as follows:

- presenting an analysis of V2V energy sharing for better EV integration and exploring its impacts on the grid.
- designing bidirectional interleaved single-phase, two-phase, and three-phase converters (buck/boost) for flexible V2V charging and discussing their application specific operation modes.
- analyzing the interleaved converters in terms of input current ripple.
- presenting the closed-loop current controller design and their respective simulation results.
- verifying the operation by performing hardware experiments for single- and two-phase boost/buck interleaved converters.

Section II of this paper presents a system analysis of the proposed V2V CSN operation. Section III presents three possible power electronics design approaches to the problem. Section IV presents the simulation results and explains the closed-loop control. Section V presents the results on the test bench. Lastly, Section VI provides the concluding remarks and the planned future work.

II. Analysis of V2V Energy Sharing and Possible Impacts in Power System Operation

We developed a Java-based simulation tool to analyze and verify the viability of the proposed V2V CSN technology [15] and to show its impact on grid operation. As an example to the prospective benefits of V2V CSN, Fig. 2 shows a possible scenario of how V2V charging can be dispatched to result in load-shifting services within a larger vehicle grid integration (VGI) framework. The developed tool generates customized simulation environment with different parameters including EV types and counts, charging station types and locations, and user mobility patterns. We used the locations of Level 2 (L2) charging stations in the Dallas metro area as a baseline case study and assumed different number and types of EVs. Using realistic battery charge levels of users and commuting patterns, we analyzed the potential V2V CSN in comparison to the scenario with only L2 stations.

Relevant to V2V CSN analysis, we only provide here some motivating simulation results as the main focus of this paper is to further investigate required power electronics. In Fig. 3, we show the number of V2V chargers and L2 charging stations used to supply the demand with increasing EV counts. We assume that only a maximum of 10% of EVs participate in the V2V CSN as a V2V charger (actual number of V2V chargers used could be smaller). The graph shows that even though the demand grows with increasing number of EVs, the V2V chargers can sustain the demand while the number of L2 stations used stabilizes. This shows that without building L2 charging stations, with the support of V2V chargers, the

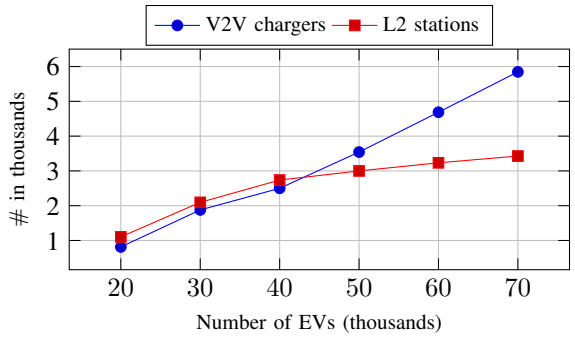

Fig. 3. Number of V2V chargers vs. L2 stations used to supply demand with increasing EV counts.

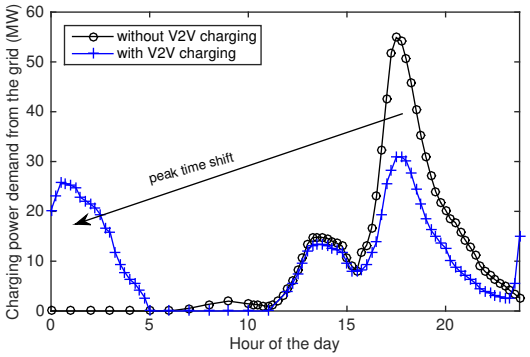

Fig. 4. Distribution of charging power demands from the grid with and without V2V charging.

growing demand could be sustained. Therefore, such a system could yield larger number of EVs operating in the area without new L2 station installations.

We also obtain the change in the daily charging power from the grid with and without V2V charging. As it is shown in Fig. 4, the peak time demand could be shifted towards night using V2V suppliers. These V2V suppliers charge themselves during night and supply receivers during the day. In this specific setting, V2V charging effectively reduces the peak charging load by 44% reducing the stress on the system.

Different grid services, such as charging when renewable generation is high, will be investigated as a future study. That is, supplier EVs will receive incentives to charge during the times when renewable generation (i.e. wind and solar), which is intermittent in nature, is high. This will in turn impact the scheduling of charging events of supplier EVs.

III. Analysis of V2V Energy Transfer Using DC-DC Converters

The dc-dc converter topologies investigated in this paper are non-isolated as there is no grid connection requirement. Three candidate solutions to this operation reported for similar applications in the literature known as bidirectional (interleaved) dc-dc converters are shown in Fig. 5 [22], [27], [28]. Each V2V charger solution presented in Fig. 5 consists of a power stage with an appropriate set of gate-drive circuits, a digital signal processor (DSP), voltage sensing circuits to measure the local EV battery voltages (V_1, V_2), and one current sensor to measure the real-time phase current (I_{La}). The DSP will

TABLE I
Operation Modes of Vehicle #1 and #2

Voltage	Mode	S_{a1}	S_{a2}	S_{a3}	S_{a4}
$V_1 > V_2$	Buck-12	Active	SR	ON	OFF
$V_1 < V_2$	Boost-12	ON	OFF	SR	Active
$V_1 > V_2$	Boost-21	SR	Active	ON	OFF
$V_1 < V_2$	Buck-21	ON	OFF	Active	SR

TABLE II
Duty cycle and inductor current ripple in continuous boost and buck operation modes

	Boost converter	Buck converter
Duty cycle (d)	$1 - \frac{V_{in}}{V_{out}}$	$\frac{V_{out}}{V_{in}}$
Inductor current ripple (Δi_L)	$\frac{V_{in} \cdot d}{f_s \cdot L}$	$\frac{V_{out} \cdot (1-d)}{f_s \cdot L}$

communicate with the vehicles via CAN through a data link embedded in the charging cable to coordinate the two ends. The direction of charge transfer will be determined by the on-board DSP.

The charger has four separate operational modes, identified in Table I for the sample case of single-phase conversion (Fig. 5(a)). Since the buck and boost mode cannot occur at the same time, only one phase-leg operates at switching mode while the other is in static mode. For instance, referring to Fig. 5(a), there is one switch which is actively modulating the flow of power between the vehicles (active) and one switch which is operating as a synchronous rectifier (SR). The remaining two switches are fixed in a constant state (ON/OFF) to statically attach the sink (buck mode) or source (boost mode).

In multiple phase operation as shown in Fig. 5(b) and (c) the switching signal for the parallel, active switches is shifted by T/N where T is the switching period, and N is the number of parallel phases. This operation is called interleaving. Interleaving the dc-dc converter brings in advantages in terms of reducing passive filter requirements at the expense of more circuit complexity [29], [30]. Another advantage is that the peak phase current reduces with interleaving. Therefore, maximum average power that can be transferred to the receiver battery increases for a given semiconductor device.

The reduction of the current ripple can be seen at the input (V_1 in Fig. 5) during boost mode or at the output (V_2 in Fig. 5) during buck mode. Table II provides the equations for the duty cycle and the resulting current ripple seen at a single inductor for boost and buck operation. The current ripple at one inductor not only depends on the operating mode but also on the switching frequency and inductance value. Another approach for reducing the current ripple is to increase the switching frequency or inductance. However, increasing the inductance usually is not desired for a compact and flexible V2V charger. Table III further shows how the current ripple reduces depending on the number of parallel phases and the duty cycle.

A baseline analysis for the converter operation is done using a switching frequency of 20 kHz and L_a=L_b=L_c=262 μH. The operating point is chosen at V_{in}=250 V and V_{out}=300 V

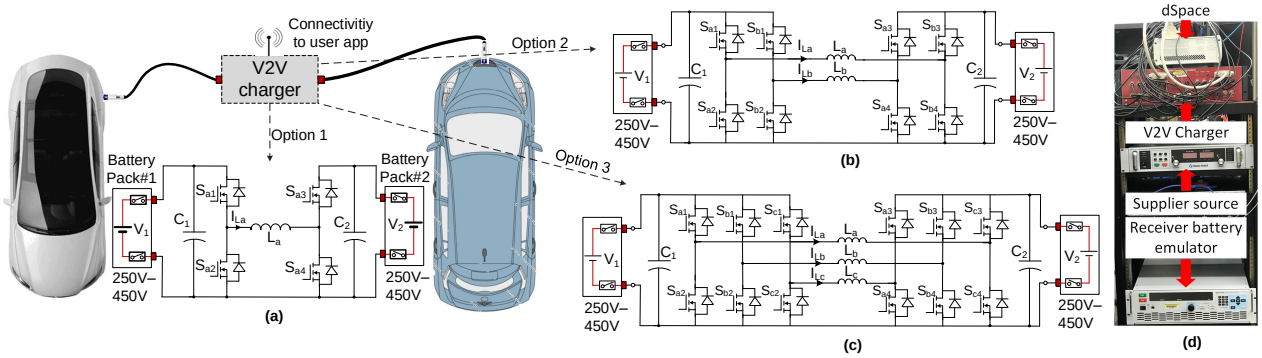

Fig. 5. Bidirectional DC-DC converters for V2V charger: a) single-phase, b) two-phase, c) three-phase and d) hardware set-up.

TABLE III
TOTAL RIPPLE CURRENT IN CONT. BOOST & BUCK OPERATIONS [31], [32]

Configuration	Duty ratio	Ripple of $\sum I_L$
Single-phase	$0 < d < 1.0$	Δi_L
Two-phase	$0 < d < 0.5$	$\Delta i_L \cdot (\frac{1-2d}{1-d})$
Two-phase	$0.5 < d < 1$	$\Delta i_L \cdot (\frac{2d-1}{d})$
Three-phase	$0 < d < 0.33$	$\Delta i_L \cdot (\frac{1-3d}{1-d})$
Three-phase	$0.33 < d < 0.66$	$\Delta i_L \cdot \{\frac{(1-3d)\cdot(3d-2)}{3d\cdot(1-d)}\}$
Three-phase	$0.66 < d < 1$	$\Delta i_L \cdot (\frac{3d-2}{d})$

for the boost mode and V_{in}=300 V and V_{out}=250 V for the buck mode. The reasoning behind choosing these values is to stay within the same rating region with the experimental setup which is detailed in Section V. However, similar analysis results can be obtained for higher voltage levels as the new EV battery voltage levels tend to have higher values. Fig. 6 shows the analysis results for the ripple current for the selected values. As the input and output voltage levels get closer to each other, the amount of the current ripple reduction becomes smaller and interleaving gets less attractive. Assuming a 50 V voltage difference between supplier EV and receiver EV (which can be a good starting point based on the current EV battery voltage data), there is a current ripple reduction of 20% for two-phase operation and 40% for three-phase operation compared to single-phase. However, as the voltage difference decreases, this reduction is less pronounced making interleaving less attractive. This analysis approach will be similar to higher pack voltages as well.

It is also important to note that the maximum value of battery current ripple is defined by the EV charging/discharging standards at 5% of the charging/discharging nominal current or 5 A whichever is lower [33], [34]. During a charging/discharging session, the on-board battery management system (BMS) monitors the current ripple, and when is above the standard limit, the BMS triggers an alert in the EV dashboard stopping the charging session. The charger should always stay away from entering this faulty operation mode further emphasizing the importance of current ripple calculations presented here.

IV. SIMULATION RESULTS WITH CLOSED-LOOP CONTROLLER DESIGN

We developed a Simulink model for single, two-phase, and three-phase boost and buck converter topologies. The model operates with a close-loop control with the sum of the inductor currents as control variable. The reason behind this selection is to clearly control the power or supplied current between the two EVs. However, this can also be done by only sensing and feeding back one inductor current. The controlled duty cycle to inductor current transfer functions are given as follows:

$$G_{id}^{boost}(s) = \frac{2V_{out}}{(1-D)^2R} \cdot \frac{1+s\frac{RC}{2}}{1+s\frac{L}{(1-D)^2R}+s^2\frac{LC}{(1-D)^2}}$$
$$G_{id}^{buck}(s) = \frac{V_{out}}{DR} \cdot \frac{1+sRC}{1+s\frac{L}{R}+s^2LC} \quad (1)$$

A unity gain for the controller would be enough to get a stable closed-loop response even though the current dynamics of both systems are too fast. However, we design PI controllers to slow down the response and remove the steady-state error as shown below:

$$G_{PI}(s) = K_p(1+\frac{K_i}{s}) \quad (2)$$

The PI coefficients used in this study are $K_p = 4.1624{\cdot}10^{-6}$ and $K_i = 247686.81$ for boost converter, and $K_p = 6.65014 \cdot 10^{-6}$ and $K_i = 350005.50$ for buck converter. The coefficients

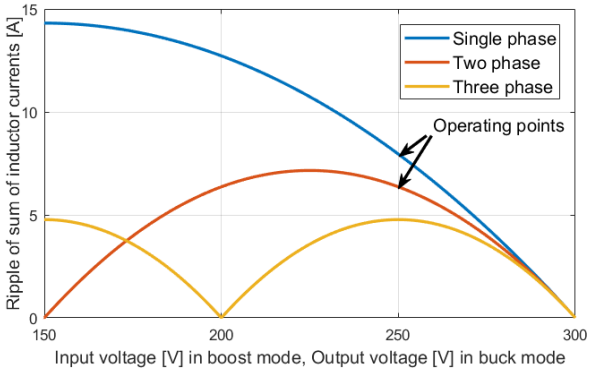

Fig. 6. Ripple of sum of inductor currents ($f_s = 20\ kHz$, inductance $L_a = L_b = L_c = 262\ \mu H$, $V_{out} = 300\ V$ in boost mode, and $V_{in} = 300\ V$ in buck mode).

are tested and verified in simulations for single, two- and three-phase configurations and the results are demonstrated in Fig. 7 for boost, and in Fig. 8 for buck. They present the simulation results at the previously mentioned operating points. The inductor currents are shown for different commanded mean values, to verify the closed-loop operation. Note that the current ripple is independent of the mean current as long as the mean current is high enough to operate in continuous mode. These controller coefficients are also used in the actual controller running on dSPACE MicroLabBox for hardware experiment which is detailed in the next section.

V. Experimental Test Results

This section explains the experimental verification of the proposed method. For this, a special purpose built back-to-back inverter system and dSPACE MicroLabBox are used as illustrated in Fig. 9. The back-to-back inverter system is composed of a dual three-phase inverter ready to be interfaced with dSPACE MicroLabBox development system. This system is rated at 10 kW with the maximum switching frequency of 20 kHz and a maximum input/output voltage of 750 VDC. For the three-phase modules, APTGT50A120T1G IGBTs from Microsemi with SP1 package is used. As for the passive components, a 260 μH inductor for each phase and a 100 μF film capacitor for the output are used. The dSpace MicroLabBox functions as the electronics control module where all high-level and low-level controllers are executed. The algorithms used are developed in MATLAB Simulink, and the execution code is generated via real time code generation. For the emulation of the supplier battery, a 10 kW MagnaPower XR series power supply is used. For the receiver battery, a 2.5 kW ALx Series MagnaLOAD DC electronic load is used via controlling it in the constant voltage mode. The real hardware rack set-up is also shown in Fig. 5(d).

The hardware system is tested for both boost and buck operations for single- and two-phase interleaved typologies. We were not able to test three-phase topology with the available dSPACE controller due to not having access to 120° phase-shifted PWM generation. V_1=250 V and V_2=300 V are chosen as battery voltage levels of supplier and receiver vehicles for boost mode, and V_1=300 V and V_2=250 V are selected for buck mode of operation. These voltage levels are relatively

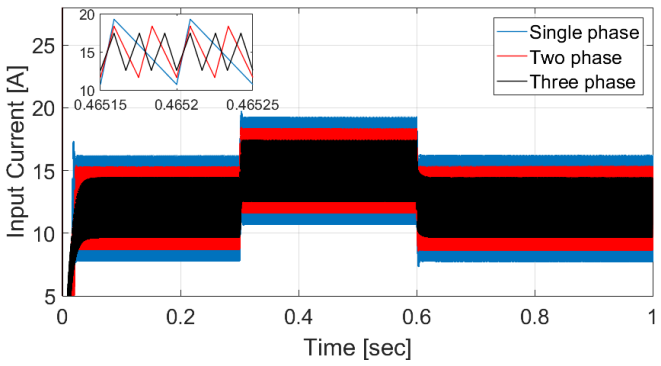

Fig. 7. Simulation results of input currents for single-, two- and three-phase interleaved boost converters.

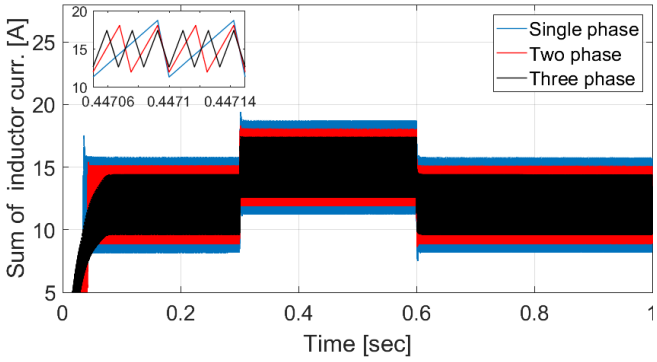

Fig. 8. Simulation results of sum of inductor currents for single-, two- and three-phase interleaved buck converters.

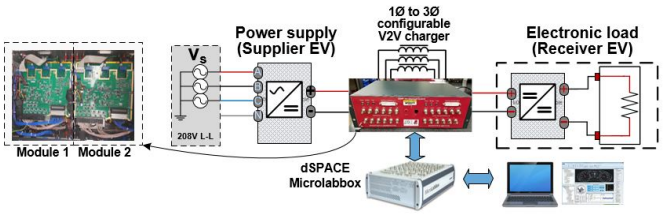

Fig. 9. V2V charging system test set-up.

low compared to battery pack voltages of today, however, they are intentionally set low to have a wide range over the controlled current without exceeding the power limits of the electronic load. The switching frequency is set to be 20 kHz for all operations, and T_s =0.05 ms is used for the closed-loop controller and data acquisition sampling period. For both operations (boost and buck), the sum of the inductor currents is controlled for consistency, and to better observe the impact of additional phases.

Fig. 10 (a) and (b) depict the input and output current and voltage waveforms for single and two-phase boost converters, respectively. The effective switching frequency seen from the input is doubled due to the additional phase. This results in a 26.31% decrease in the input current ripple for the two-phase design compared to the single phase one. Fig. 11 (a) and (b) show the current and voltage waveforms for single and two-phase buck converters, respectively. We observe the same effective frequency for the buck converter, and as a result the ripple current reduces by 30%.

Table IV summarizes the test results and compares them with the calculation results. There is a slight difference between the experimental and theoretical results. Our set-up is current controlled, thus the actual operating duty ratio is going to be slightly different every time we change our commanded current due to non-ideal measurements. However, we can see that the actual ripples are in line with the calculated ones.

TABLE IV
Experimental results for current ripple values.

	Boost conv. ripple (A)		Buck conv. ripple (A)	
	Calculation	Experiment	Calculation	Experiment
Single phase	7.95	7.6	7.95	6.6
Two-phase	6.36	5.6	6.36	4.6
Three-phase	4.77	-	4.77	-

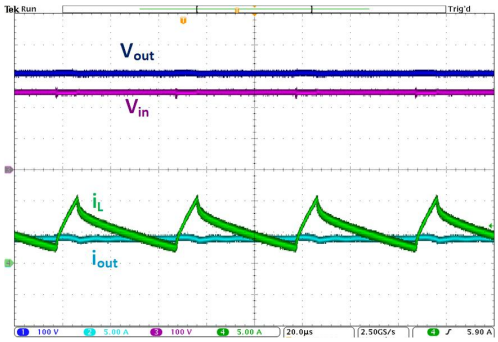

(a)

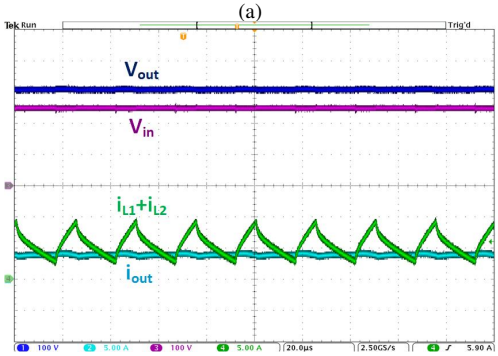

(b)

Fig. 10. Comparison of (a) single and (b) two-phase boost mode of operation results (V_{in} and V_{out}: 100 V/div, i_L and i_{out}: 5 A/div, and t: 20 μs/div).

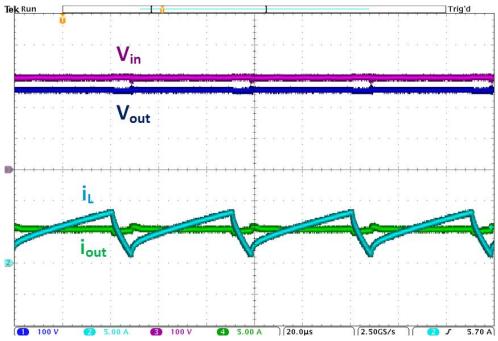

(a)

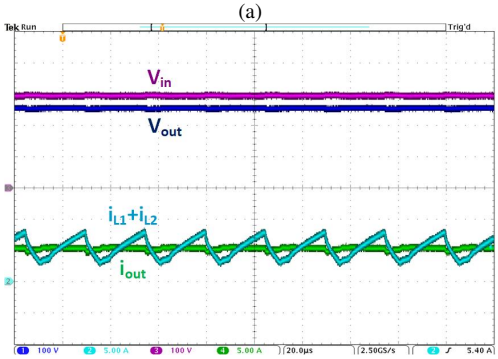

(b)

Fig. 11. Comparison of (a) single and (b) two-phase buck mode of operation results, (V_{in} and V_{out}: 100 V/div, i_L and i_{out}: 5 A/div, and t: 20 μs/div))

To test the performance of the closed-loop controller designed in Chapter IV, we commanded different current values as our reference. The resulting currents are recorded at the sampling frequency of 20 kHz and demonstrated along with the reference current in Fig. 12 (a) and (b) for the boost single

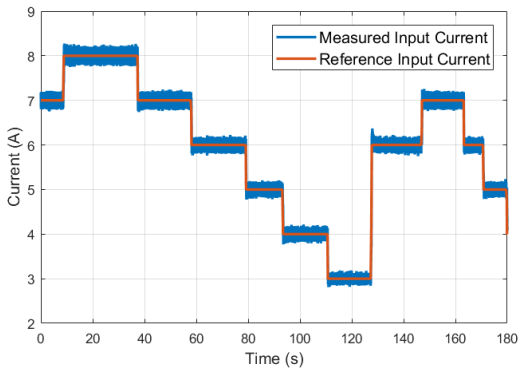

(a)

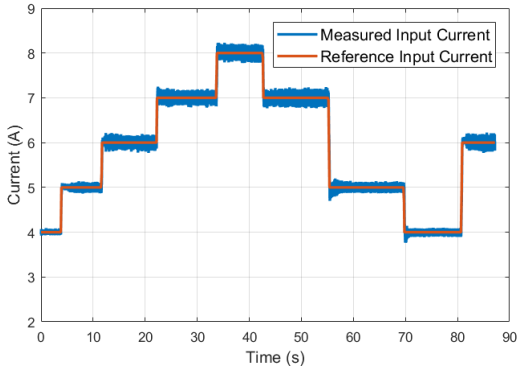

(b)

Fig. 12. Comparison of measured and reference current to verify closed-loop control in (a) single-phase and (b) two-phase boost mode

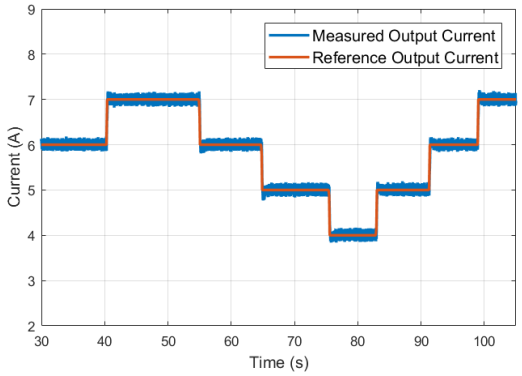

(a)

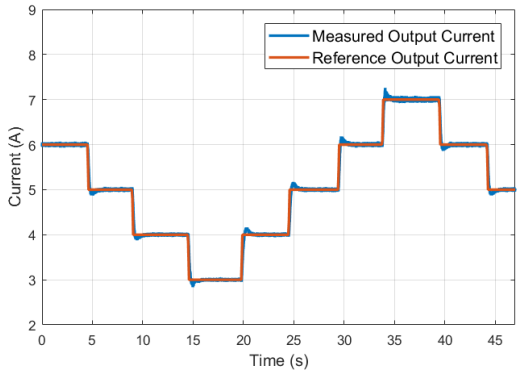

(b)

Fig. 13. Comparison of measured and reference current to verify closed-loop control in (a) single-phase and (b) two-phase buck mode

and two-phase, and in Fig. 13 (a) and (b) for the buck single and two-phase converters. As seen, the controller works stable and the system follows the commanded currents. We see that the experimental results verify our theoretical and simulation results in that the current ripple is being reduced by each additional phase. The amount of reduction depends on the duty ratio (operating point), and it gets significantly smaller as the battery voltages get closer to each other, and vice versa.

VI. Conclusions

This study envisions the viability of an EV-to-EV energy sharing using compact and flexible charging infrastructure. Such infrastructure will help and facilitate widespread penetration of EVs into the market reducing the reliance on expensive and non-ubiquitous DCFC infrastructure. The overall merit of this study lies in the design of a V2V charger to be used in CSN. The study presents the design of a compact bidirectional two-way buck/boost DC-DC converter to provide a proof of concept for energy transfer between two different battery packs of any typical voltage level. We analyzed three candidate options to transfer energy between two wide battery voltage levels and compared their advantages. A significant improvement in inductor ripple current is observed when multi-phase bidirectional dc-dc converters are used as opposed to the single-phase counterpart at the expense of increased complexity. Future work will involve a high power density and efficient design of the V2V charger. We will also investigate its impact on grid integration along with more renewable energy generation.

References

[1] E. Veldman and R. A. Verzijlbergh, "Distribution grid impacts of smart electric vehicle charging from different perspectives," *IEEE Trans. Smart Grid*, vol. 6, no. 1, pp. 333–342, 2015.

[2] L. P. Fernandez, T. G. S. Roman, R. Cossent, C. M. Domingo, and P. Frias, "Assessment of the impact of plug-in electric vehicles on distribution networks," *IEEE Trans. Power Syst.*, vol. 26, no. 1, pp. 206–213, Feb 2011.

[3] S. Shafiee, M. Fotuhi-Firuzabad, and M. Rastegar, "Investigating the impacts of plug-in hybrid electric vehicles on power distribution systems," *IEEE Trans. Smart Grid*, vol. 4, no. 3, pp. 1351–1360, 2013.

[4] F. Erden, M. C. Kisacikoglu, and O. H. Gurec, "Examination of ev-grid integration using real driving and transformer loading data," in *Int. Conf. Elect. Electron. Eng.*, 2015, pp. 364–368.

[5] E. Sortomme, M. M. Hindi, S. J. MacPherson, and S. Venkata, "Co-ordinated charging of plug-in hybrid electric vehicles to minimize distribution system losses," *IEEE Trans. Smart Grid*, vol. 2, no. 1, pp. 198–205, 2011.

[6] N. Leemput, F. Geth, J. Van Roy, A. Delnooz, J. Buscher, and J. Driesen, "Impact of electric vehicle on-board single-phase charging strategies on a flemish residential grid," *IEEE Trans. Smart Grid*, vol. 5, no. 4, pp. 1815–1822, 2014.

[7] K. Clement-Nyns, E. Haesen, and J. Driesen, "The impact of charging plug-in hybrid electric vehicles on a residential distribution grid," *IEEE Trans. Power Syst.*, vol. 25, no. 1, pp. 371–380, Feb 2010.

[8] O. Sundstrom and C. Binding, "Flexible charging optimization for electric vehicles considering distribution grid constraints," *IEEE Trans. Smart Grid*, vol. 3, no. 1, pp. 26–37, March 2012.

[9] "Global EV outlook: beyond one million electric cars," https://www.iea.org/publications/freepublications/publication/Global_EV_Outlook_2016.pdf, Tech. Rep., 2016, [Online; accessed 18-Apr-2019].

[10] W. Kempton and S. Letendre, "Electric vehicles as a new power source for electric utlilities," *Trans. Res.*, vol. 2, no. 3, pp. 157–175, 1997.

[11] (2016) Charging forward: The state of EV charging in 2016. https://www.chargepoint.com/charging-forward-2016. [Online; accessed 18-Apr-2019].

[12] N. Nigro and M. Frades, "Business models for financially sustainable EV charging networks," http://leg.wa.gov/JTC/Documents/Studies/EV/FinalReport_EVChargingNetworksWEB.pdf, Center for Climate and Energy Solutions, Tech. Rep., 2015, [Online; accessed 18-Apr-2019].

[13] J. Leeder. (2017) Ontario's electric-vehicle charging network hits speed bumps. https://www.theglobeandmail.com/news/toronto/ontarios-electric-vehicle-charging-network-hits-speed-bumps/article34441795. [Online; accessed 18-Apr-2019].

[14] (2015) Plugged in: How americans charge their electric vehicles. https://avt.inl.gov/sites/default/files/pdf/arra/PluggedInSummaryReport.pdf. [Online; accessed 18-Apr-2019].

[15] E. Bulut and M. C. Kisacikoglu, "Mitigating range anxiety via vehicle-to-vehicle social charging system," in *IEEE Veh. Tech. Conf.*, Jun. 2017.

[16] R. Zhang, X. Cheng, and L. Yang, "Flexible energy management protocol for cooperative ev-to-ev charging," *IEEE Trans. Intell. Transp. Syst.*, no. 99, pp. 1–13, 2018.

[17] F. Yucel, K. Akkaya, and E. Bulut, "Efficient and privacy preserving supplier matching for electric vehicle charging," *Ad Hoc Networks*, in press.

[18] B. Roberts, K. Akkaya, E. Bulut, and M. Kisacikoglu, "An authentication framework for electric vehicle-to-electric vehicle charging applications," in *MASS REU Res. Netw. Systems Workshop*. IEEE, 2017.

[19] S. Dusmez, A. Hasanzadeh, and A. Khaligh, "Comparative analysis of bidirectional three-level dc-dc converter for automotive applications," *IEEE Trans. Ind. Electron.*, vol. 62, no. 5, pp. 3305–3315, May 2015.

[20] O. Garcia, P. Zumel, A. de Castro, and A. Cobos, "Automotive dc-dc bidirectional converter made with many interleaved buck stages," *IEEE Trans. Power Electron.*, vol. 21, no. 3, pp. 578–586, May 2006.

[21] T. J. C. Sousa, V. Monteiro, J. C. A. Fernandes, C. Couto, A. A. N. Melendez, and J. L. Afonso, "New perspectives for vehicle-to-vehicle (V2V) power transfer," in *Annual Conf. IEEE Ind. Electron. Soc.*, Oct 2018, pp. 5183–5188.

[22] M. O. Badawy, M. N. Arafat, A. Ahmed, S. Anwar, Y. Sozer, P. Yi, and J. A. D. Abreu-Garcia, "Design and implementation of a 75-kw mobile charging system for electric vehicles," *IEEE Trans. Ind. Appl.*, vol. 52, no. 1, pp. 369–377, Jan 2016.

[23] M. Nasr, K. Gupta, C. da Silva, C. H. Amon, and O. Trescases, "SiC based on-board EV power-hub with high-efficiency DC transfer mode through AC port for vehicle-to-vehicle charging," in *IEEE Applied Power Electron. Conf. Expo. (APEC)*, 2018, pp. 1–7.

[24] (2018) Andromeda Power. www.andromedapower.com. [Online; accessed 18-Apr-2019].

[25] (2019) Uber. www.uber.com. [Online; accessed 20-Apr-2019].

[26] Mark Kane. (2017) https://insideevs.com/here-is-how-nissan-leaf-can-rescue-stranded-tesla-model-s/. [Online; accessed 18-Apr-2019].

[27] B. Vural, S. Dusmez, M. Uzunoglu, E. Ugur, and B. Akin, "Fuel consumption comparison of different battery/ultracapacitor hybridization topologies for fuel-cell vehicles on a test bench," *IEEE J. Emerg. Sel. Topics Power Electron.*, vol. 2, no. 3, pp. 552–561, Sept 2014.

[28] Y. Du, X. Zhou, S. Bai, S. Lukic, and A. Huang, "Review of non-isolated bi-directional dc-dc converters for plug-in hybrid electric vehicle charge station application at municipal parking decks," in *IEEE Applied Power Electron. Conf. Expo. (APEC)*, Feb 2010, pp. 1145–1151.

[29] C. Chang and M. A. Knights, "Interleaving technique in distributed power conversion systems," *IEEE Trans. Circuits Syst. I, Fundam. Theory Appl.*, vol. 42, no. 5, pp. 245–251, May 1995.

[30] M. Gerber, J. A. Ferreira, I. W. Hofsajer, and N. Seliger, "Interleaving optimization in synchronous rectified dc/dc converters," in *IEEE Power Electronics Specialists Conf. (PESC)*, vol. 6, June 2004, pp. 4655–4661.

[31] D. Baba, "Under the hood of a multiphase synchronous rectified boost converter," https://www.ti.com/seclit/wp/slup323/slup323.pdf, Texas Instruments, Tech. Rep., 2014, [Online; accessed 18-Apr-2019].

[32] C. Parisi, "Multiphase buck design from start to finish(part1)," http://www.ti.com/lit/an/slva882/slva882.pdf, Texas Instruments, Tech. Rep., 2017, [Online; accessed 18-Apr-2019].

[33] "Road vehicles-vehicle to grid communication interface," *ISO/IEC Standard 15118*, 2013.

[34] Chademo protocol- EV fast standard. https://www.chademo.com. [Online; accessed 26-Apr-2019].